

Electrochemical impedance spectroscopy study of high-palladium dental alloys. Part I: Behavior at open-circuit potential*

D. SUN

Section of Oral Biology, College of Dentistry, The Ohio State University, Columbus, OH, USA

P. MONAGHAN, W. A. BRANTLEY,† W. M. JOHNSTON

Section of Restorative Dentistry, Prosthodontics and Endodontics, College of Dentistry, The Ohio State University, PO Box 182357, Columbus, OH, USA 43218-2357

E-mail: brantley.1@osu.edu

Electrochemical impedance spectroscopy (EIS) was used to study the *in vitro* corrosion of three representative high-palladium alloys and a gold–palladium alloy for comparison. The corrosion resistances (measured as the charge transfer resistance R_{CT} from an equivalent circuit) of the high-palladium alloys and the gold–palladium alloy were comparable in simulated body fluid and oral environments, and under simulated dental plaque. The great similarity in corrosion behavior for the three high-palladium alloys is largely attributed to their substantial palladium content and passivity in the laboratory test media, and possibly to their similar structure at the submicron level. Differences in composition and microstructure at the micron level and greater, including the effects of heat treatment simulating the firing cycles for dental porcelain, do not have noteworthy effects on the *in vitro* corrosion of the three high-palladium alloys. Good accuracy and convenience of extracting corrosion characteristics from equivalent circuit modeling, along with the capability of providing intrinsic information about the corrosion mechanism, enable EIS to be an excellent alternative method to conventional potentiodynamic polarization for evaluating the corrosion behavior of noble dental alloys.

© 2002 Kluwer Academic Publishers

1. Introduction

High-palladium casting alloys containing greater than 75 wt % palladium, and derived from the Pd–Cu–Ga and Pd–Ga systems, are popular alternatives to traditional gold-based alloys for metal-ceramic restorations in restorative dentistry [1,2], because of their excellent mechanical properties [3,4] and good porcelain adherence [5]. Corrosion of the cast alloy may result in failure of the restoration and biocompatibility problems due to ion release [6]. Moreover, while definitive explanations are lacking, some health problems attributed to the use of palladium alloys for dental restorations have been reported [7,8]. Elucidation of the corrosion behavior and mechanisms for high-palladium alloys helps provide a better understanding of their biocompatibility, which in turn may result in the development of improved dental casting alloys.

Conventional potentiodynamic polarization methods, originally used to study *in vitro* corrosion of gold-based casting alloys [9–13], have also been extensively used to investigate the corrosion behavior of the high-palladium

dental alloys. The corrosion behavior of the latter alloys in media-simulating body fluids and the oral environment is excellent and comparable to that of the gold-based alloys [13–18]. Recent research has shown that the *in vitro* corrosion behavior of representative high-palladium alloys in the as-cast and simulated porcelain-firing heat-treated conditions is essentially equivalent [19]. Whereas some previous studies with older palladium-based alloys concurred that heat treatment, microstructures and compositions did not affect corrosion behavior [20–22], contradictory results have also been reported [23–25].

The excellent corrosion resistance of the high-palladium alloys has been attributed to their passivity and the inherent nobility of palladium [19]. Both the Pd–Cu–Ga and Pd–Ga alloys, either as-cast or after simulated porcelain-firing cycles, exhibited spontaneous passive behavior for *in vitro* conditions representative of the oral environment [19]. Atomic absorption and X-ray photoelectron spectroscopy revealed that selective dissolution of Co and Cu occurred for binary Pd–Co

*A part of this study was presented at the 30th annual meeting of the American Association for Dental Research, Chicago, IL, March 2001.

†Author to whom all correspondence should be addressed.

and Pd–Cu alloys in an artificial saliva, resulting in a palladium-enriched surface [26]. Sarkar and colleagues [24, 27–29] have employed potentiodynamic polarization methods to show that the *in vitro* corrosion behavior differs for silver-containing and silver-free high-palladium alloys. Formation of silver-enriched surfaces for the former and palladium-enriched surfaces for the latter has important implications about their biocompatibility.

While potentiodynamic polarization methods provide information concerning corrosion resistance and susceptibility, passivation behavior, and energetic considerations for film breakdown, they cannot be used to study the interfacial phenomena that govern the corrosion process. Moreover, because information is obtained far from steady-state conditions, reaction rates for *in vivo* conditions may not be determined accurately and, at elevated potentials compared to the corrosion potential, diffusion of species often limits the interfacial reactions. Electrochemical impedance spectroscopy (EIS) [30–32] uses very small amplitude signals that minimally perturb the electrodes. Additionally, EIS provides the capabilities of studying corrosion reactions, measuring corrosion rates, and determining multiple corrosion parameters that govern charge transfer and charge storage from the same measurement.

The objective of this study was to investigate and compare the *in vitro* corrosion behavior of three high-palladium alloys and a gold–palladium alloy with a relatively long history of acceptable clinical performance, by the combined use of potentiodynamic polarization and EIS. Equivalent circuit models were developed for each alloy to fit the EIS data and explain the contributions of certain processes to the overall electrochemical properties.

2. Materials and methods

Two Pd–Cu–Ga alloys, Freedom Plus (78Pd–8Cu–5Ga–6In–2Au) [wt %] and Liberty (76Pd–10Cu–5.5Ga–6Sn–2Au), and one Pd–Ga alloy, Legacy (85Pd–10Ga–1In–2Au–1Ag), were selected for this study. A gold–palladium alloy, Olympia (51.5Au–38.5Pd–8.5In–1.5Ga), with an extensive history of excellent clinical performance was included for comparison to the high-palladium alloys. All four alloys are marketed by the same manufacturer (J. F. Jelenko & Co., Armonk, NY, USA).

Disk-shaped alloy castings of 12 mm diameter and 1.3 mm thickness were prepared by standard dental laboratory procedures [1, 2]. After removal of the casting investment, each specimen was wet-ground on both sides with 180, 400 and 600 grit silicon carbide abrasive papers, and polished with 5, 1, 0.3 and 0.05 μm alumina slurries. After polishing, each specimen was ultrasonically cleaned in both distilled water and ethanol for 10 min, respectively.

Corrosion tests were performed for both the as-cast and heat-treated conditions of each alloy in three different electrolytes: 0.09% and 0.9% NaCl solutions, whose chloride concentrations are similar to those in human saliva and body fluids, respectively, and Fusayama solution [33], an artificial saliva. Heat treatment simulated the firing cycles [3] for Vita VMK

dental porcelain (Vident, Baldwin Park, CA, USA). The heat-treated specimens of each alloy were also tested in two other electrolytes, N_2 -deaerated 0.09% NaCl solution (pH = 4) and N_2 -deaerated Fusayama solution (pH = 4), which were chosen to simulate clinical conditions at the metal–environment interface under oral bacterial plaque [34, 35]. Citric acid was used to adjust the pH value of the latter two solutions. A 2.5 cm \times 2.5 cm platinum plate served as the counter electrode, and a saturated Ag|AgCl reference electrode was used.

After immersion in an electrolyte for 24 h at room temperature, the EIS test [31, 32] was performed on an alloy specimen. During this test, a ± 10 mV sinusoidal voltage varying around the previously determined [36] corrosion potential (E_{CORR}) [37] was impressed upon the specimen over the range of 10 kHz to 0.01 Hz, with 10 points per decade (PC4 potentiostat and CMS 100 software, Gamry Instruments, Inc., Warminster, PA, USA). The current was collected and analyzed for magnitude and phase relationship with the voltage, to determine the electrochemical impedance of the system. The sample size used with the EIS tests was five for each alloy/condition (as-cast or heat-treated) and electrolyte combination. Commercially available software (Zview, Scribner Associates, Inc., Southern Pines, NC, USA) was used to model the EIS data.

A linear polarization test was also performed for each specimen in the same conditions (as-cast or heat-treated alloy and the particular electrolyte) as those for the EIS tests. Each specimen was polarized in the range of ± 20 mV around the open-circuit potential (OCP) [36], using a scanning rate of 0.125 mV/sec. The polarization resistance [32, 37] (designated as one measure of the corrosion resistance) for each alloy condition was determined by linear regression and compared with a second measure of the corrosion resistance obtained from equivalent-circuit modeling [37] of the EIS data. After being used in one experiment, each specimen was polished again and reused in another test.

The mean values of the corrosion resistances of all four alloys for both the as-cast and heat-treated conditions, as appropriate, in each electrolyte were compared by two-way analysis of variance (ANOVA), using a statistical software package (SAS Institute Inc., Cary, NC, USA) at a significance level of $\alpha = 0.05$. The Ryan–Einot–Gabriel–Welsch (REGW) multiple range test ($\alpha = 0.05$) was used to determine specific cases of statistical significance for these parameters.

3. Results

3.1. EIS spectra at open-circuit potential and equivalent circuit modeling

Figs. 1–5 are representative EIS spectra for the three high-palladium alloys (Freedom Plus, Legacy and Liberty) and the gold–palladium alloy (Olympia) in the five electrolytes (0.9% NaCl, 0.09% NaCl, Fusayama, deaerated 0.09% NaCl and deaerated Fusayama solutions). The specimens for these figures were in the clinically relevant heat-treated condition simulating the firing cycles for dental porcelain [5]. The top of each figure contains the Nyquist diagrams [32] showing the

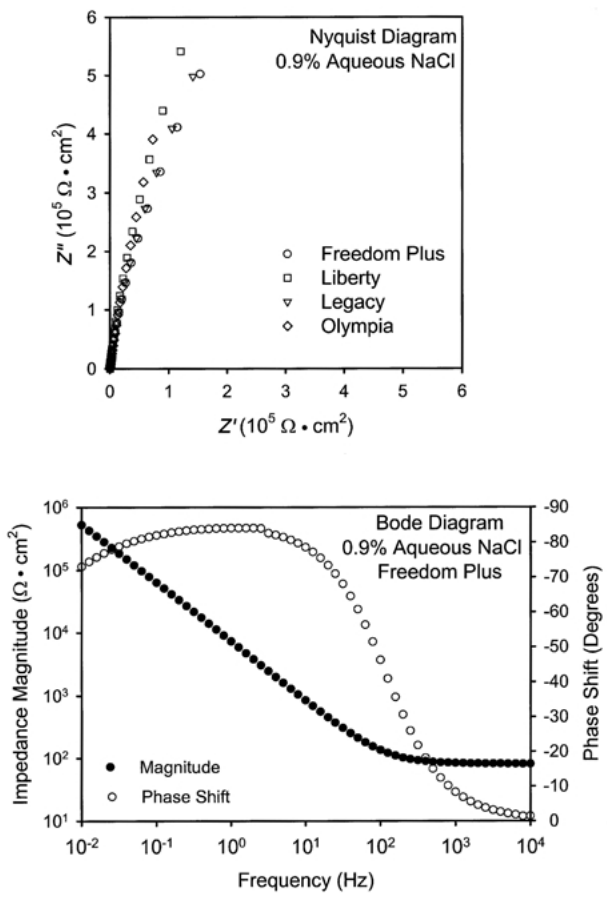


Figure 1 Nyquist diagrams for all four heat-treated alloys and Bode diagram for Freedom Plus in 0.9% NaCl solution.

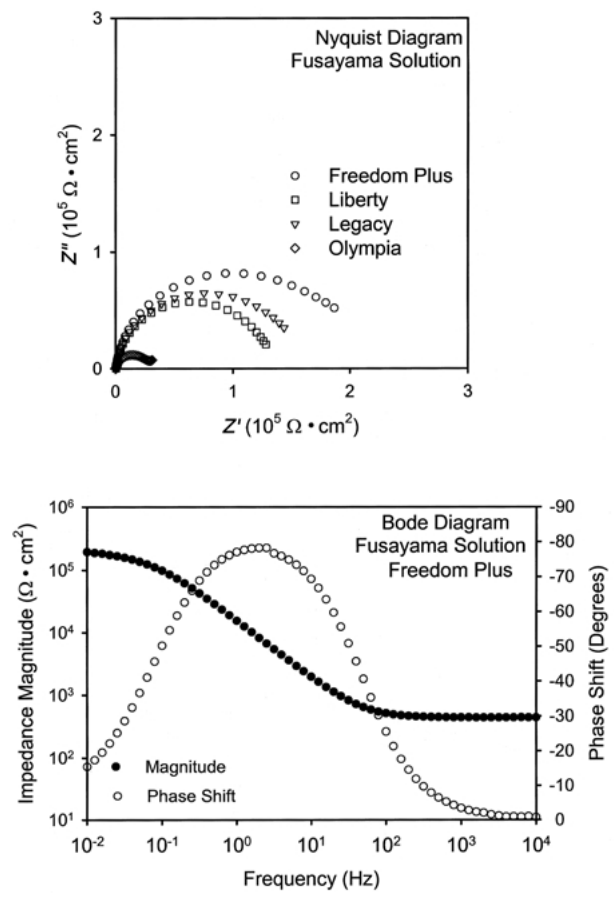


Figure 3 Nyquist diagrams for all four heat-treated alloys and Bode diagram for Freedom Plus in Fusayama solution.

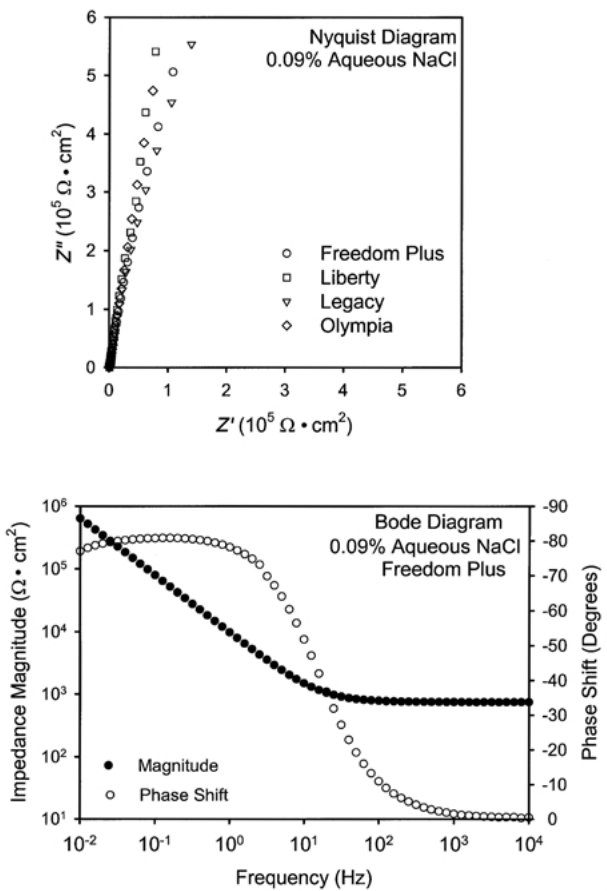


Figure 2 Nyquist diagrams for all four heat-treated alloys and Bode diagram for Freedom Plus in 0.09% NaCl solution.

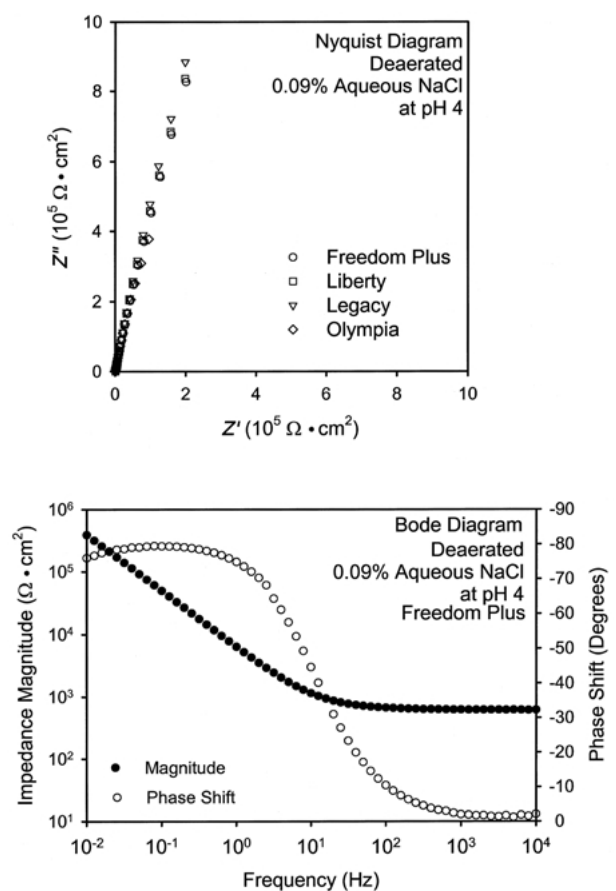


Figure 4 Nyquist diagrams for all four heat-treated alloys and Bode diagram for Freedom Plus in deaerated 0.09% NaCl solution (pH = 4).

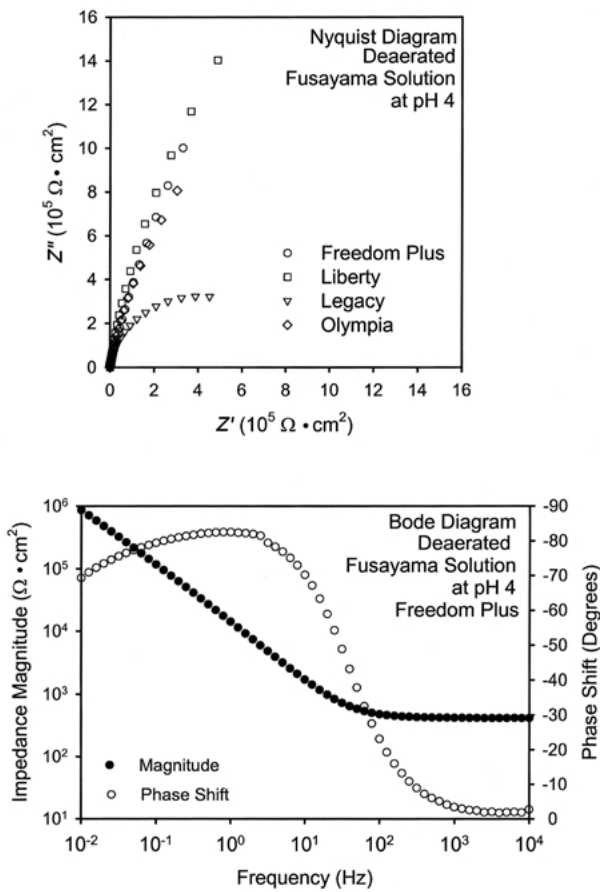


Figure 5 Nyquist diagrams for all four heat-treated alloys and Bode diagram for Freedom Plus in deaerated Fusayama solution (pH = 4).

relationship between complex (out-of-phase) impedance (Z'') and real (in-phase) impedance (Z') for the four alloys. The Bode log-log plots [32] of impedance magnitude and phase shift as a function of frequency are shown for only one alloy (Freedom Plus) in the bottom part of each figure, since the Bode plots for all four alloys in this study would be indistinguishable on the same graph. The EIS spectra of these alloys for the as-cast condition were almost identical to their counterparts for the heat-treated condition. Comparison of the spectra for the five different specimens from the same alloy in the same electrolyte revealed good reproducibility.

The best equivalent circuit for the EIS spectra of the alloys is a Randles-like model, designated as $R_S - R_{CT} - CPE$, in which the polarization charge-transfer resistance (R_{CT}) is in parallel with a constant phase element (CPE), and both of these elements are in series with the ohmic resistance R_S , as shown in Fig. 6. In this model, the constant-phase element may have some combination of capacitive, resistive and inductive character [32].

In Fig. 6, R_S is the total ohmic resistance of the electrochemical cell and contains contributions from the solution, cables and other sources. R_{CT} is considered to be the corrosion resistance of the alloy, which is inversely proportional to the corrosion current density. The CPE is defined by two parameters, T and P , in the equation for impedance [38, 39]

$$Z = \frac{1}{T(j\omega)^P}$$

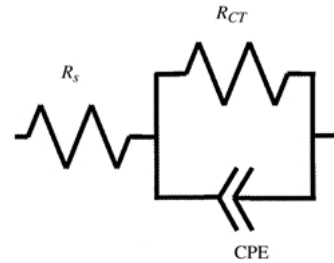


Figure 6 Equivalent Randles-like circuit model for EIS results.

The value of the exponent P may vary from 0 to 1. If P equals 1, then the CPE is a capacitor. If P equals 0, then the CPE is a resistor. A CPE is often used in an equivalent circuit model in place of a capacitor to compensate for inhomogeneity in the system. For example, a rough or porous surface can be modeled by a constant phase element with a P value between 0.9 and 1 [40], instead of a capacitance.

3.2. Corrosion resistance of high-palladium alloys

The R_{CT} , T and P values of all four alloys for both the as-cast and heat-treated conditions in each electrolyte are listed in Table I. Generally, the R_{CT} , T and P values of the three high-palladium alloys are comparable to those for the gold-palladium alloy, Olympia.

In Fig. 7, the polarization resistances determined from linear polarization (R_p) and from the equivalent modeling (R_{CT}) are compared for the high-palladium alloys. (The data for the Olympia groups have been excluded because of very high mean values and standard deviations for R_{CT} .) When $R_{CT} < 2 \times 10^6 \Omega \text{ cm}^2$, the R_{CT} and R_p values agree with each other relatively well, i.e., in the same order of magnitude. However, when $R_{CT} > 2 \times 10^6 \Omega \text{ cm}^2$, R_{CT} and R_p can differ by up to three orders of magnitude, and R_p is always much less than R_{CT} .

4. Discussion

4.1. Interpretation of EIS Spectra

For the electrolytes and the experimental conditions of the present study, the EIS spectra of the three high-palladium alloys and the gold-palladium alloy can generally be modeled as a Randles-like ($R_S - R_{CT} - CPE$) equivalent circuit (Fig. 6). This shows that the *in vitro* corrosion of these alloys in the simulated body fluid and the simulated oral environment was basically under charge transfer control. However, Olympia in 0.09% NaCl and deaerated 0.09% NaCl (pH = 4) solutions (Figs. 2 and 4) was found to have very high R_{CT} values. This suggests that the charge transfer process is highly inhibited by the formation of a stable double layer for heat-treated Olympia in the 0.09% NaCl and deaerated

TABLE I EIS parameters (R_{CT} , T and P values) of the tested alloys*

| Alloy | Treatment | $R_{CT} (\times 10^6 \Omega \text{ cm}^2)$ | | $T \times 10^{-6} (\Omega^{-1} \text{ cm}^{-2} \text{ rad}^{-P})$ | P |
|---|--------------|--|---|---|-------------------|
| <i>0.9% NaCl solution</i> | | | | | |
| Freedom Plus | As-cast | 1.622 ± 0.732 | A | 27.30 ± 3.31 | 0.911 ± 0.028 |
| Freedom Plus | Heat-treated | 3.044 ± 0.652 | A | 23.56 ± 2.67 | 0.928 ± 0.024 |
| Liberty | As-cast | 7.068 ± 0.148 | A | 15.10 ± 1.86 | 0.906 ± 0.009 |
| Liberty | Heat-treated | 4.682 ± 0.926 | A | 22.80 ± 1.57 | 0.934 ± 0.005 |
| Legacy | As-cast | 24.020 ± 36.524 | A | 14.12 ± 2.96 | 0.903 ± 0.015 |
| Legacy | Heat-treated | 3.064 ± 1.014 | A | 23.06 ± 3.39 | 0.933 ± 0.007 |
| Olympia | As-cast | $1.94 \times 10^8 \pm 2.66 \times 10^8$ | A | 33.88 ± 8.46 | 0.874 ± 0.012 |
| Olympia | Heat-treated | 7.611 ± 4.811 | A | 37.28 ± 4.36 | 0.915 ± 0.007 |
| <i>0.09% NaCl solution</i> | | | | | |
| Freedom Plus | As-cast | 1.986 ± 1.256 | A | 22.88 ± 4.10 | 0.890 ± 0.013 |
| Freedom Plus | Heat-treated | 6.870 ± 2.211 | A | 20.00 ± 3.02 | 0.909 ± 0.010 |
| Liberty | As-cast | 15.964 ± 7.808 | A | 18.54 ± 2.51 | 0.907 ± 0.009 |
| Liberty | Heat-treated | 13.603 ± 9.631 | A | 20.00 ± 1.07 | 0.919 ± 0.005 |
| Legacy | As-cast | 12.190 ± 4.188 | A | 15.52 ± 2.81 | 0.896 ± 0.021 |
| Legacy | Heat-treated | 5.706 ± 6.049 | A | 26.92 ± 11.76 | 0.884 ± 0.051 |
| Olympia | As-cast | $6.48 \times 10^7 \pm 9.66 \times 10^7$ | B | 33.16 ± 8.64 | 0.864 ± 0.026 |
| Olympia | Heat-treated | N/A | | 50.98 ± 26.18 | 0.871 ± 0.064 |
| <i>Fusayama solution</i> | | | | | |
| Freedom Plus | As-cast | 0.214 ± 0.192 | A | 13.46 ± 1.93 | 0.917 ± 0.018 |
| Freedom Plus | Heat-treated | 0.197 ± 0.0714 | A | 13.28 ± 1.12 | 0.907 ± 0.014 |
| Liberty | As-cast | 0.0311 ± 0.148 | A | 18.76 ± 10.97 | 0.888 ± 0.042 |
| Liberty | Heat-treated | 0.102 ± 0.0452 | A | 14.24 ± 1.75 | 0.911 ± 0.012 |
| Legacy | As-cast | 6.292 ± 6.090 | B | 12.78 ± 0.73 | 0.928 ± 0.013 |
| Legacy | Heat-treated | 0.167 ± 0.120 | A | 27.64 ± 10.60 | 0.819 ± 0.066 |
| Olympia | As-cast | 0.140 ± 0.0850 | A | 42.76 ± 27.48 | 0.836 ± 0.046 |
| Olympia | Heat-treated | 0.0285 ± 0.00469 | A | 33.44 ± 13.63 | 0.843 ± 0.049 |
| <i>Deaerated NaCl solution (pH=4)</i> | | | | | |
| Freedom Plus | Heat-treated | 12.135 ± 5.997 | A | 14.05 ± 0.99 | 0.890 ± 0.009 |
| Liberty | Heat-treated | 32.636 ± 38.120 | A | 15.58 ± 3.05 | 0.891 ± 0.010 |
| Legacy | Heat-treated | 218.520 ± 397.897 | A | 69.00 ± 109.08 | 0.766 ± 0.233 |
| Olympia | Heat-treated | N/A | | 39.18 ± 26.05 | 0.878 ± 0.033 |
| <i>Deaerated Fusayama solution (pH=4)</i> | | | | | |
| Freedom Plus | Heat-treated | 5.174 ± 0.639 | A | 9.71 ± 0.40 | 0.900 ± 0.009 |
| Liberty | Heat-treated | 5.428 ± 0.511 | A | 8.56 ± 0.75 | 0.932 ± 0.010 |
| Legacy | Heat-treated | 1.713 ± 1.855 | A | 12.28 ± 1.57 | 0.910 ± 0.016 |
| Olympia | Heat-treated | $1.58 \times 10^7 \pm 3.53 \times 10^7$ | A | 18.48 ± 7.57 | 0.905 ± 0.024 |

*Entries are mean \pm standard deviation ($N=5$). For each electrolyte, mean values of R_{CT} with different letters were significantly different, using the REGW test ($p=0.05$).

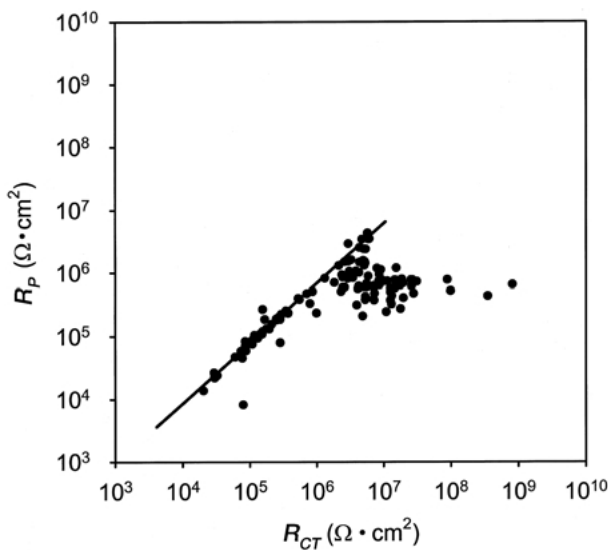


Figure 7 Comparison of values of corrosion resistance determined from linear polarization (R_p) and EIS modeling (R_{CT}) for the high-palladium alloys.

0.09% NaCl (pH = 4) solutions, and by the high nobility of this Au–Pd alloy.

Casting defects [41] produce inhomogeneous surfaces that can affect the corrosion behavior of alloys. Porosity, inclusions and carbon contamination in cast high-palladium alloys have been described [42–44]. Hot tears have also been found in castings of some high-palladium alloys with dendritic microstructures [45], although all the alloys used in the present study had equiaxed, fine-grained microstructures. Another casting defect that can occur in high-palladium alloys is excessive carbon contamination, which arises from use of a graphite crucible or a poorly adjusted torch [43]; however, only dedicated ceramic crucibles were used for fusing the alloys in this study. Inclusions in the cast alloys can originate from investment debris or from the metallurgical polishing process. Scanning electron microscope examination at moderate magnifications ($\times 100$) of the specimens used in this study revealed surface defects, such as those described above, that

would contribute to the observed electrochemical activity of each alloy.

Microstructural effects might cause deviation from ideal capacitive behavior in the corrosion of the high-palladium alloys. Multiple phases at or near the surface have been observed in high-palladium alloys [2, 46], and selective corrosion of different phases and/or less noble metals has been found in palladium-based alloys [24, 26]. Tufekci *et al.* [47] investigated the elemental release from two representative heat-treated high-palladium alloys, Liberty (Pd–Cu–Ga) and Legacy (Pd–Ga), after immersion in an aqueous lactic acid/NaCl solution for 7, 70 and 700 h. Pd, Cu, Ga, Sn, In and Ru were detected for at least one immersion time, while the concentrations of any Au and Ag released were below the detection limit at any time period. For Liberty, palladium may be released from dissolution of the Pd₂Ga phase and the solid solution matrix, based upon the ratio of the concentrations of the released Pd and Ga. This selective corrosion of different metallurgical phases in the heat-treated high-palladium alloys would account for their non-ideal electrochemical activity in the present experiments.

Palladium is a surface-active metal and is often used as a catalyst [48, 49]. Adsorption of oxygen or hydrogen from the electrolytes and polymeric components from the mucin in the Fusayama solution may occur for the high-palladium alloys, and this would make the electrochemical interface inhomogeneous during the EIS testing. Moreover, chloride ions, found in all electrolytes used in this study, cause the oral environment to be quite corrosive [11] and have a detrimental effect on the surface of the high-palladium alloys [11, 50].

The ability to model all of the EIS spectra for the high-palladium alloys in the five electrolytes to an R_S – R_{CT} –CPE equivalent circuit can be attributed to their high noble metal content (palladium and gold) and possibly to their microstructures. Although there are multiple phases in each alloy and heat treatment can result in microstructural changes viewed in the scanning electron microscope, the tweed structure was shown by transmission electron microscopy (TEM) to be the dominant structural constituent at the submicron level in the high-palladium alloys for both the as-cast and heat-treated conditions [51, 52]. It is plausible that this tweed structure contributes to the similar corrosion behavior for the high-palladium alloys that have been evaluated, but further research is needed to verify this hypothesis.

4.2. Factors influencing the corrosion of high-palladium alloys

The composition and microstructure (affected by whether an appropriate post-casting heat treatment is performed), and the electrolyte used for testing, can have profound effects on the corrosion behavior of an alloy. The R_{CT} values for the three high-palladium alloys and the gold-palladium alloy, Olympia, in the five electrolytes are provided in Table I. For all of the testing conditions, only one specimen group for the three high-palladium alloys (as-cast Legacy in the Fusayama solution) and only one specimen group for the Olympia alloy (as-cast, 0.09% NaCl solution) had significantly different values for R_{CT} . The reasons why these two

specimen groups had significantly different *in vitro* corrosion resistance remain to be established, although unknown differences in surface structure would be a plausible explanation. Other potentiostatic polarization studies have also found great similarity in the corrosion properties for different high-palladium alloys [6–8].

The effects of heat treatment on corrosion resistance can be associated with the resulting microstructural changes. However, in the present study, no significant differences in R_{CT} values were generally detected between the as-cast and heat-treated conditions for all four alloys in the five electrolytes (Table I), presumably because of their high inherent corrosion resistance. (The two exceptions were Olympia and Legacy in the as-cast condition.) In particular, the corrosion resistance of the high-palladium alloys in the deaerated 0.09% NaCl and Fusayama solutions (both with pH=4) was not significantly different from that in the 0.09% NaCl and Fusayama solutions which had not been deaerated. From these results, one would predict that, even in such rigorous oral conditions as under dental plaque, the corrosion resistance of these high-palladium alloys is not significantly decreased. Consequently, these alloys should and do have an excellent record of clinical performance.

It is not surprising that all three high-palladium alloys have similar corrosion characteristics in the present study, since it was previously found [19] that composition, microstructure and heat treatment have only minor effects on the corrosion behavior of these alloys. As noted previously, the high palladium content in these alloys and their very similar structure at the submicron level [51, 52] are presumed to be the origin of their similar corrosion behavior. Sarkar and colleagues have suggested that *in vitro* corrosion of the high-palladium alloys yields a palladium-enriched surface [24, 27–29]. This conclusion and the speculation by Nitta *et al.* [52] that the tweed structure of the high-palladium alloys has high stability and is resistant to corrosion attack require further research for verification.

The mean R_{CT} values for each alloy in Fusayama solution are less than those in the 0.09% and 0.9% NaCl solutions for the same condition (Table I). This is consistent with the results from our complementary potentiodynamic polarization study of these alloys [53]. Holland [12] studied the effects of different electrolytes on the potentiodynamic polarization results obtained for various dental alloys and found that an aqueous 1% NaCl solution, which is very close to the 0.9% NaCl solution in the present study, is more corrosive than the Fusayama solution. This deviation from the results of the present study is assumed to arise from the different alloy compositions evaluated and differences between the EIS and potentiodynamic polarization test methods. Hence, care is required when comparing the corrosion characteristics of dental alloys obtained with different electrolytes and test methods.

4.3. Comparison of two methods to evaluate corrosion resistance

The values of corrosion resistance (R_{CT}) of the high-palladium alloys determined from the EIS method

correlate well with values of polarization resistance (R_p) obtained from linear polarization [53], when $R_{CT} < 2 \times 10^6 \Omega \text{ cm}^2$ (Fig. 8). This good correlation shows that EIS is a very useful method to characterize the corrosion behavior of high-palladium and gold-palladium dental alloys. EIS not only provides a value (R_{CT}) for the corrosion resistance of the alloys, but also yields information about the corrosion mechanisms. Minor differences in the corrosion resistance values can arise from experimental errors for the two methods or from the modeling process. While the R_S - R_{CT} -CPE model is not a perfect Randles-like model, the values of R_{CT} obtained from this modeling are certainly related to the corrosion resistance of the materials. Since the use of a CPE in the model means that the double layer between the corroding metal surface and the electrolyte is not an ideal capacitor [32], some other electrochemical processes whose effects are included in the CPE may also account for the interfacial activity. Fortunately, the P values in the models are very close to 1, so that the corrosion resistance from this equivalent circuit modeling is still quite accurate.

The deviation of corrosion resistance from these two methods becomes substantial when $R_{CT} > 2 \times 10^6 \Omega \text{ cm}^2$. This may arise from the extrapolation of the EIS spectra to lower frequencies than those used in the present study to obtain the R_{CT} values. The linear polarization was performed in the range of $\pm 20 \text{ mV}$ around E_{CORR} [37], using a scanning rate of 0.125 mV/sec , so that the R_p values were obtained at a very low frequency of 0.003125 Hz (quotient of 0.125 mV/sec and 40 mV). For the frequency range used in the present study, the *in vitro* corrosion of all of the alloys tested is under capacitive process control [32] (Figs. 1–6), and thus the R_{CT} values obtained by extrapolation can cause a large deviation between the R_{CT} and R_p values, especially when R_{CT} is high. The correct R_{CT} values can only be obtained when much lower testing frequencies are used than the lowest frequency of 0.01 Hz in the present study. However, it is difficult to attain such low frequencies in the laboratory, and the corrosion parameters might change during the long test period. (For example, 5 min are required for one cycle at 0.003125 Hz .) In the present experiments, the R_p value from linear polarization never exceeded $10^7 \Omega \text{ cm}^2$, whereas R_{CT} values approaching $10^9 \Omega \text{ cm}^2$ were obtained (Fig. 7). The lower maximum values of R_p from linear polarization measurements, compared to the maximum values of R_{CT} obtained from EIS modeling, might be due to limitations of the equipment and software for the linear polarization experiments, as well as the appropriateness of the modeling used for the complex corrosion processes in these noble dental alloys.

5. Conclusions

The corrosion resistances of three representative high-palladium alloys evaluated by both EIS and linear polarization methods are comparable to those of a high-noble, gold-palladium alloy in simulated body fluid and oral environments, and under simulated plaque. This *in vitro* result is consistent with the excellent clinical performance of the high-palladium alloys and the

gold-palladium alloy. The great similarity between the three high-palladium alloys in corrosion behavior can be attributed to their high palladium content and very similar structures at the submicron level. Differences in composition and microstructure of these high-palladium alloys, including the effects of heat treatment, do not have substantial effects on their *in vitro* corrosion.

The accuracy and convenience of extracting corrosion characteristics from equivalent circuit modeling, along with providing intrinsic information about the corrosion mechanism, enable EIS to be a good alternative to potentiodynamic methods for evaluating the corrosion behavior of noble dental alloys. The intrinsic information about the corrosion mechanisms obtained from EIS is useful for improved understanding of the biocompatibility of these alloys.

Acknowledgments

Support for this research was received from Grant DE10147, National Institute of Dental and Craniofacial Research, Bethesda, MD, USA, and from a University Faculty Seed Grant. We thank Professor Gerald S. Frankel, Department of Materials Science and Engineering, The Ohio State University for helpful comments during this study and manuscript preparation.

References

1. A. B. CARR and W. A. BRANTLEY, *Int. J. Prosthodont.* **4** (1991) 265.
2. W. A. BRANTLEY, Z. CAI, A. B. CARR and J. C. MITCHELL, *Cells Mater.* **3** (1993) 103.
3. E. PAPAZOGLU, Q. WU, W. A. BRANTLEY, J. C. MITCHELL and G. MEYRICK, *ibid.* **9** (1999) 43.
4. E. PAPAZOGLU, Q. WU, W. A. BRANTLEY, J. C. MITCHELL and G. MEYRICK, *J. Mater. Sci.: Mater. Med.* **11** (2000) 601.
5. E. PAPAZOGLU, W. A. BRANTLEY, A. B. CARR and W. M. JOHNSTON, *J. Prosthet. Dent.* **70** (1993) 386.
6. J. C. WATAHA, R. G. CRAIG and C. T. HANKS, *J. Dent. Res.* **70** (1991) 1014.
7. Z. CAI, X. CHU, S. D. BRADWAY, E. PAPAZOGLU and W. A. BRANTLEY, *Cells Mater.* **5** (1995) 357.
8. J. C. WATAHA and C. T. HANKS, *J. Oral Rehabil.* **23** (1996) 309.
9. N. K. SARKAR, R. A. FUY, JR and J. W. STANFORD, *J. Dent. Res.* **58** (1979) 568.
10. R. I. HOLLAND, R. B. JØRGENSEN and H. HERØ, *Dent. Mater.* **2** (1986) 143.
11. R. I. HOLLAND, *Scand. J. Dent. Res.* **99** (1991) 75.
12. R. I. HOLLAND, *Dent. Mater.* **8** (1992) 241.
13. J.-M. MEYER and L. RECLARU, *J. Mater. Sci.: Mater. Med.* **6** (1995) 534.
14. J. LANE, L. LUCAS, W. LACEFIELD, J. O'NEAL and J. LEMONS, *J. Dent. Res.* **64** (1985) 318 (Abstr. No. 1291).
15. P. R. MEZGER, M. M. A. VRIJHOEF and E. H. GREENER, *Dent. Mater.* **1** (1985) 177.
16. P. R. MEZGER, M. M. A. VRIJHOEF and E. H. GREENER, *J. Dent. Res.* **65** (1986) 748 (Abstr. No. 199).
17. S. VERMILYEA, N. MANOGARAN and W. A. BRANTLEY, *ibid.* **74** (1995) 237 (Abstr. No. 1806).
18. N. K. MANOGARAN, S. G. VERMILYEA and W. A. BRANTLEY, *ibid.* **74** (1995) 241 (Abstr. No. 1833).
19. Z. CAI, S. G. VERMILYEA and W. A. BRANTLEY, *Dent. Mater.* **15** (1999) 202.
20. P. R. MEZGER, M. M. A. VRIJHOEF and E. H. GREENER, *J. Dent.* **17** (1989) 33.
21. K. BÖNING and M. WALTER, *Int. Dent. J.* **40** (1990) 289.

22. C. MÜLDERS, M. DARWISH and R. HOLZE, *J. Oral Rehabil.* **23** (1996) 825.
23. D. BERZINS, N. K. SARKAR and I. KAWASHIMA, *J. Dent. Res.* **78** (1999) 112 (Abstr. No. 54).
24. I. KAWASHIMA, D. BERZINS, N. K. SARKAR and A. PRASAD, *ibid.* **78** (1999) 236 (Abstr. No. 1045).
25. L. JOSKA and M. MAREK, *ibid.* **79** (2000) 596 (Abstr. No. 3619).
26. V. GOEHLICH and M. MAREK, *Dent. Mater.* **6** (1990) 103.
27. D. BERZINS, N. K. SARKAR, I. KAWASHIMA and H. OHNO, *J. Dent. Res.* **79** (2000) 596 (Abstr. No. 3617).
28. D. W. BERZINS, I. KAWASHIMA, R. GRAVES and N. K. SARKAR, *Dent. Mater.* **16** (2000) 266.
29. N. K. SARKAR, D. W. BERZINS and A. PRASAD, *ibid.* **16** (2000) 374.
30. F. MANSFELD, *Corrosion* **36** (1981) 301.
31. EG&G Princeton Applied Research, Princeton, NJ. Application Note AC-1 (1985). "Basics of electrochemical impedance spectroscopy (EIS)".
32. W. S. TAIT, "An Introduction to Electrochemical Corrosion Testing for Practicing Engineers and Scientists", (Pair O Docs Publications, Racine, WI, 1994) pp. 79 and 95.
33. T. FUSAYAMA, T. KATAYORI and S. NOMOTO, *J. Dent. Res.* **42** (1963) 1183.
34. R. M. STEPHAN, *ibid.* **23** (1944) 257.
35. P. LINGSTRÖM, F. O. J. VAN RUYVEN, J. VAN HOUTE and R. KENT, *ibid.* **79** (2000) 770.
36. D. SUN, Master of Science thesis, The Ohio State University, Columbus, OH, USA (2000).
37. M. G. FONTANA, "Corrosion Engineering", 3rd edn. (McGraw-Hill, New York, 1986) p. 499.
38. I. D. RAISTRICK, J. R. MACDONALD and D. R. FRANCESCHETTI, in "Impedance Spectroscopy", edited by J. R. MACDONALD (Wiley, New York, 1987) p. 27.
39. Gamry Instruments, Warminster, PA. Application Notes, in "The Basics, Electrochemical Impedance Spectroscopy: A Primer", (Gamry Instruments, Warminster PA, 2000).
40. F. MANSFELD, H. SHIH, H. GREENE and C. H. TSAI, in "Electrochemical Impedance: Analysis and Interpretation", edited by J. R. Scully, D. C. Silverman and M. W. Kendig (ASTM STP 1188, American Society for Testing and Materials, Philadelphia, 1993) p. 37.
41. R. W. PHILLIPS, "Skinner's Science of Dental Materials", 9th edn. (Saunders, Philadelphia, 1991) p. 434.
42. Z. CAI, Master of Science thesis, The Ohio State University, Columbus, OH, USA (1992).
43. H. HERØ and M. SYVERUD, *Dent. Mater.* **1** (1985) 106.
44. J. M. VAN DER ZEL and M. M. A. VRIJHOEF, *J. Oral Rehabil.* **15** (1988) 163.
45. A. B. CARR, Z. CAI, W. A. BRANTLEY and J. C. MITCHELL, *Int. J. Prosthodont.* **6** (1993) 233.
46. Q. WU, W. A. BRANTLEY, J. C. MITCHELL, S. G. VERMILYEA, J. XIAO and W. GUO, *Cells Mater.* **3** (1997) 161.
47. E. TUFEKCI, J. C. MITCHELL, J. W. OLESIK, W. A. BRANTLEY, E. PAPAZOGLU and P. MONAGHAN, *J. Prosthet. Dent.* **87** (2002) 80.
48. A. N. CORREIA, L. H. MASCARO, A. S. MACHADO and L. A. AVACA, *Electrochim. Acta* **42** (1997) 493.
49. T. H. YANG, S. I. PYUN and Y. G. YOON, *ibid.* **42** (1997) 1701.
50. K. SHAN-SHIH, T. K. VAIDYANATHAN and J. VAIDYANATHAN, *J. Dent. Res.* **62** (1983) 688 (Abstr. No. 345).
51. Z. CAI, W. A. BRANTLEY, W. A. T. CLARK and H. O. COLIJN, *Dent. Mater.* **13** (1997) 365.
52. S. V. NITTA, W. A. T. CLARK, W. A. BRANTLEY, R. J. GRYLLS and Z. CAI, *J. Mater. Sci.: Mater. Med.* **10** (1999) 1.
53. D. SUN, P. MONAGHAN, W. A. BRANTLEY and W. M. JOHNSTON, *J. Prosthet. Dent.* **87** (2002) 86.

*Received 12 September
and accepted 10 October 2001*